Adaptive Self-Protective Motion based on Reflex Control

Toshihiko Shimizu, Ryo Saegusa, Shuhei Ikemoto, Hiroshi Ishiguro, Giorgio Metta

Abstract— **This paper describes a self-protective whole-body control method for humanoid robots. A set of postural reactions are used to create whole-body movements. A set of reactions is merged to cope with a general falling down direction, while allowing the upper limbs to contact safely with obstacles. The collision detection is achieved by force sensing. We verified that our method generates the self-protective motion in real time, and reduced the impact energy in multiple situations by simulator. We also verified that our systems works adequately in real-robot.**

I. Introduction

The humanoid robot iCub[1] is intended to develop its cognitive skills through physical interaction with its environments. There are many possible ways to perform this role, but for achieving life-long learning, the robot should interact with the environments safely for preventing the robot itself from being damaged. An essential point for achieving a safe interaction is the ability to react adequately to harmful situations, such as falling down during walking as shown in Fig.1. In this paper, we propose a whole-body control method for generating self-protective motion which is biologically inspired by the reflex, that is the innate function to react to an environmental stimulus instantaneously.

In robotics, Subsumption architecture[2] proposed by Brooks is known as one of the best reflex systems with high adaptability against a variety of environments. In his approach, a robot interacts with the environments by selecting the reflexes related to current the sensor information. The robot controlled by this system quickly reacts to the stimulus from external world, and its behaviors is variable because its actions are connected to differences in its environment. In this aspect, many researchers focused on the reflex-based control. Nakamura[3] proposed the reflex based walking system that adapts to the unexpected noises of environment such as a step or a force from outside. Boone[4] also proposed a bipedal walking system that is able to adapt to slipping or tripping surfaces. However, current robotic researches are mainly focused on stabilizing the robot for keeping walking or balancing, and there are few researches that focused on the self-protective reflex control for whole body motions. Thus in this paper, we tackle this problems by reflex-like control.

The proposed system consists of the following features.

- The self-protective motions aimed at absorbing the impact of falling down depending on the protecting priority.
- Collision detection in each arms adapt to the environmental uncertainties, such as obstacles.
- Local reflexes elicited by collision detection work for dumping the end-effectors impact energy.

In this paper, we verify the efficiency of the proposed system in both simulation and real-robot experiments.

Toshihiko Shimizu, and Hiroshi Ishiguro are with Department of Systems Innovation Graduate School of Engineering Science of Osaka University.

Shuhei Ikemoto is with the Department of Multimedia Engineering Graduate School of Information Science and Technology of Osaka University.

R. Saegusa, and G. Metta are with the Department of Robotics, Brain and Cognitive Sciences, Italian Institute of Technology, Genoa, Italy.

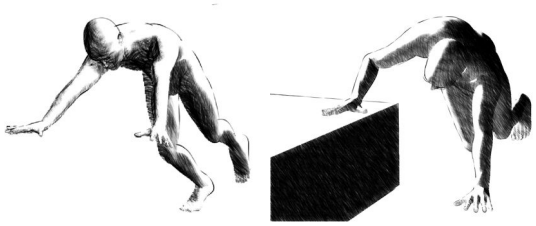

Fig. 1. Self protective motions during falling down.

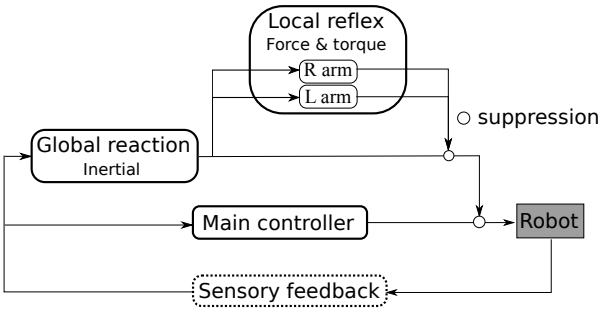

Fig. 2. The control diagram of the proposed system.

II. Reflex based self-protective motion

Fig.2 shows the control diagram of the proposed system. The system keeps observing the sensory information of normal controller such as the module for stabilizing standing or jumping, and the normal controller is suppressed when the falling down is occurred. The global reaction module suppresses the main controller output until the falling down is ended. The system generates the self-protective global reaction toward the major direction of falling down by superposing base motions, which are modified on their upper limb part depending on the environment's conditions that are perceived by the collision detection system.

A. Global reaction

In harmful situations it is sometimes impossible to ensure the whole bodies safeness, thus the robot has to protect itself depending on the protection priority of the body parts, head, torso, the limbs. By following this priority, we implemented three base motions for self-protective motion as shown in Fig.3. Base motions consists of the following features:

Fig. 3. Base motions. Right, front, left base motion from left to right.

- Upper limbs are extended toward the major direction of falling down.
- Lower limbs are flexed.
- The neck is flexed backward.

The first feature is for the protection priority. The end-effectors such as upper or lower limbs should contact first for protecting more higher priority parts, such as head and torso. The second feature comes from the aim of dissipating the impact force when the robot falls over[5]. Since the impact force comes from the potential energy that is proportional to the height of robot's center of gravity, the squatting motion can dissipate the potential energy by the damping torque generated at the lower limbs joints which have low priority. The third feature also comes from the protection priority, and aims at keeping the head safe by adapting its movement to the falling direction. The right (left) base motion are basically same as the front base motion, but the torso is twisted to right (left), and upper limbs are turned to the ground direction more than that in the front base motion. Thus, both motions are expected to work properly just like front base motion.

In order to generate a global reaction that is adequate to the major direction of falling down, base motions are used for linear super position as:

$$\theta = \sum_{k=1}^{n} w(k)\vec{\theta}(k), \tag{1}$$

where w is the weight of the motion and bounded as $\sum_{k=1}^{n} w(k) = 1$, $\vec{\theta}(k)$ is the joint angles of the kth base motions.

B. Local reflex

When the global reaction is elicited, occasionally the moving paths of the limbs are interrupted by obstacles. If the obstacles have the heavy mass, the collision occurred by following the path could damage the robot. Therefore, the global reaction should be modified adequately depending on the environment condition, especially the collision occurrence.

We implemented the local reflexes for adapting the collision, tonic reflex and flex reflex. Tonic reflex simply keeps its joint angles when the collision occurs, as the human strains their muscles to adjust the stiffness of the joints to keeps their posture. Flex reflex are bending its joints angles when the collision occurs toward the torso, for damping the impact energy like squatting motion of front base motion. These reflexes only works for the limbs, and partially modify the global reaction reflex motions.

These two reflexes are elicited by the collision detection system. The collision detection system keeps observing the sensor information until the global reaction is achieved. Once the collision is detected, the system elicits the local reflexes, the limbs are stopped or flexed. Thanks to the ability of stopping and flexing, we expect the local reflex to be efficient in adopting to environmental uncertainties.

C. Collision detection

Mohammad[6] proposed the Robust Singular Spectrum Transform (RSST), which is available for noisy data sequences without any ad-hoc tuning. Change detection method has the advantage that less prior knowledge about the detection, such as the gain, is required.

At every point $x(t)$ of a time series, SST takes the difference between the past (i.e. $x(t-p)\dots x(t)$ and future (i.e. $x(t)\dots x(t+p)$) features. The past and future features at $x(t)$ are represented by the Hankel matrix $H(t)$:

$$H(t) = [seq(t-n), ..., seq(t-1)], \tag{2}$$

where $seq(t) = \{x(t-w+1), ..., x(t)\}^T$. Singular Value Decomposition (SVD) is then used to find the singular values and vectors of the Hankel Matrix by solving:

$$H(t) = U(t)S(t)V(t)^T. \tag{3}$$

Ide[7] showed that the hyper plane built by first l left singular vectors ($U_l(t)$) encodes the major directions of change in the signal. In RSST, the number of l is dynamically determined depending on the complexity of the signal. In order to calculate $l(t)$, the singular values of $H(t)$ are sorted, and the accumulated sum of them ($l_a(t)$) is checked where the tangent of $l_a(t)$ has an angle below $-\pi/4$. The singular vectors with singular values higher than this value are assumed to be caused by the genuine feature of the signal while the other directions encode the effect of noise. Past and future patterns ($l_p(t)$ and $l_f(t)$) are calculated in the same way. Each of these $l_f(t)$ singular vectors $\beta_i(t)(i \leq l_f(t))$ are projected onto the hyper plane build by the past singular vectors $U_{l_p(t)}$:

$$\alpha_i(t) = \frac{U_{l_p(t)}^T \beta_i(t)}{\|U_{l_p(t)}^T \beta_i(t)\|}(i \leq l_f(t)). \tag{4}$$

The norms of each projection vector $\alpha_i(t)$ represent the difference between each $\beta_i(t)$ and the hyper plane, because $\|\alpha_i(t)\| \leq \|\beta_i(t)\|$ is formed as shown in Fig.4. (if the $\beta_i(t)$ is on the hyper plane, $\|\alpha_i(t)\|$ becomes 1.) Thus the changes of score of each future pattern are calculated by:

$$cs_i(t) = 1 - \|\alpha_i(t)\|. \tag{5}$$

The first guess of the change score at $x(t)$ is then calculated as the weighted sum of these change scores.

$$\widehat{x}(t) = \frac{\sum_{k=1}^{l_f(t)} \lambda_i(t) cs_i(t)}{\sum_{k=1}^{l_f(t)} \lambda_i(t)}, \tag{6}$$

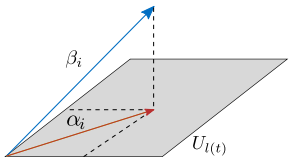

Fig. 4. Projection to the super plane build from past feature.

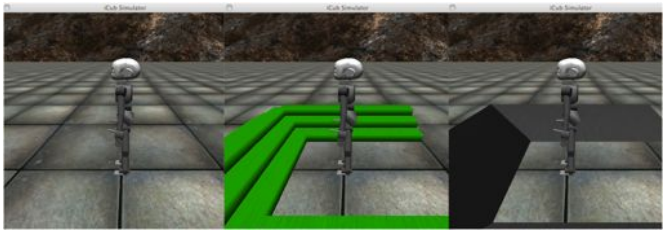

Fig. 5. Environments in iCub simulator.

where $\lambda_i(t)$ are the eigenvalues of the future feature matrix $G_f(t)$. In order to filter the effect of noise, the guess of the change score is then updated by:

$$\widetilde{x}(t) = \widehat{x}(t) \times \|\mu_f - \mu_p\| \times \|\sigma_f - \sigma_p\|, \tag{7}$$

where $\mu_p(\mu_f)$ and $\sigma_p(\sigma_f)$ are the mean and variance of a past (future) subsequence of length w at $\widehat{x}(t)$. In [6], $\widetilde{x}(t)$ are normalized by the local maximum, but we used directly $\widetilde{x}(t)$ for the online calculation.

III. Experiments

The proposed method is evaluated in both simulation and real-world robot experiment. Both experiments are conducted with iCub[1], the child-type robot designed as a three and a half year old (about 104cm tall). iCub consist of 53 degree of freedom (DOF) distributed on the head, torso, arms, hands, and legs[8]. iCub motion is controlled by a PC and iCub and PC are interconnected using YARP[9],[10]. iCub has a force torque sensor in each limb[11], thus we used these sensor information for the collision detection and elicited the local reflexes in each limb.

A. Simulation Experiment

Several environments such as flat ground, stair, slope were prepared in the iCub simulator[12]. In order to evaluate the effectiveness of the proposed system, the iCub is pushed from the back such that his torso has a linear velocity $\vec{v}_0$. As the normal control, the robot keeps standing at initial position. The global reaction is elicited when the norm of moving average of the head linear velocity exceeds $\|\vec{v}_h(t)\| \geq 0.2\,\mathrm{m/sec}$. The weights for global reaction in Eq.1 are calculated as:

$$w_f = \vec{x}_h \cdot \vec{v}_h / \|\vec{v}_h\|, \tag{8}$$

where w_f is the weight of front base motion and $\vec{x}_h$ is the x axis of the robot head coordination. The other weights are defined as:

$$w_l = \begin{cases} 0 & (\vec{v}_0^{\,y}(t) < 0) \\ 1 - w_f & (otherwise), \end{cases} \tag{9}$$

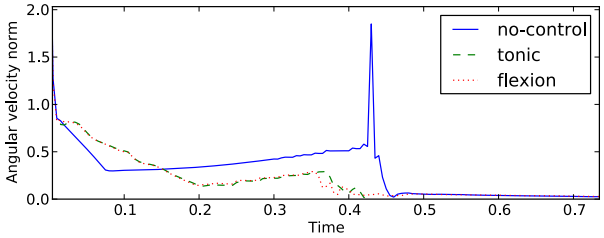

Fig. 6. The comparison of angular velocity norm on front falling down.

$$w_r = 1 - (w_f + w_l), \tag{10}$$

where w_l and w_r is the weight for left and right base motion, and $\vec{v}_0^{\,y}(t)$ is the y axis element of $\vec{v}_h(t)$.

During the global reaction, the changing score $\widehat{x}(t)$ is calculated by RSST along the all axes of iCub force torque sensor. The RSST's parameter are set to $w = 5, n = 5$, while the simulation step is set to $s = 0.005\,\mathrm{sec}$. Thus, the global reaction has a chance of being elicited every $s = 0.05\,\mathrm{sec}$, necessary for calculating the moving average, and the local reflexes has a change of being started every $s = 0.05\,\mathrm{sec}$, the time necessary for calculating the changing score. Each iCub force torque sensor has 3 axes, so the changing score $\widehat{X}(t) = \{\widehat{x}(t)_{fx}, \widehat{x}(t)_{fy}, \widehat{x}(t)_{fz}, \widehat{x}(t)_{tx}, \widehat{x}(t)_{ty}, \widehat{x}(t)_{tz}\}$ of each axis is calculated individually, and summarized by taking norm of these three score at each time t. The local reflex is elicited when $\|\widehat{X}(t)\| > 1e^{-15}$. For the flexion reflex, we set the differential angles for each motions as:

$$d\vec{\theta} = \begin{cases} \{20, 0, 0, 20\} & (w_f > 0.8) \\ \{0, -20, 0, 10\} & (otherwise), \end{cases} \tag{11}$$

where each element of $d\vec{\theta}$ is the flexing amount of shoulder pitch, roll, yaw, and elbow pitch respectively.

Here, we verify the efficiency of the proposed system to dump the impact energy when the collision occur. Here we uses the norm of angular velocity because it represents the energy of motions. We prepared several cases named right, half right, front, half left, left of falling down that has the initial push velocity $\vec{v}_o$ as $\{0, -10, 0\}$, $\{5, -5, 0\}$, $\{10, 0, 0\}$, $\{5, 5, 0\}$, $\{0, 10, 0\}\,\mathrm{m/sec}$ respectively, and 10 trials are performed for each cases to calculate the average score. The comparison between no-control and global reaction with tonic reflex and flexion reflex is shown in Table.I, and a example of of front falling down is shown in Fig.6. In each direction at every environments, the proposed system reduces the velocity norm around the impact. There are no significant differences between tonic and flexion but both works effectively.

In order to evaluate the differences between tonic and flexion reflex, we calculated the energy consumption at the joints of upper limbs, because this energy associated with the consumption energy during collision. Here we are interested in the kinematic energy, thus we define the total joint drive

TABLE I

THE COMPARISON OF THE ANGULAR VELOCITY NORM AROUND COLLISION BETWEEN NO-CONTROL AND GLOBAL REACTIONS WITH TONIC AND FLEXION REFLEX IN EACH ENVIRONMENTS.

condition \ falling down direction	right	half right	front	half left	left
	Flat environment				
no-control	13.5	12.1	11.8	15.3	16.0
global reaction with tonic	10.5	9.9	4.9	11.7	10.4
global reaction with flexion	11.1	10.2	5.6	11.9	9.8
	Slope environment				
no-control	14.1	13.1	9.4	15.6	13.8
global reaction with tonic	9.5	9.3	4.7	10.6	11.6
global reaction with flexion	10.0	10.4	4.0	9.9	10.7
	Stair environment				
no-control	11.0	26.2	11.1	12.7	12.3
global reaction with tonic	9.7	7.9	4.5	11.8	10.6
global reaction with flexion	8.9	8.1	4.1	11.6	10.1

energy rate $E(t)$ by summing up for all the joints as follows:

$$E(t) = \sum_{k=1}^{n} \dot{\theta}_i(t) T_i(t), \tag{12}$$

where $\dot{\theta}_i(t)$ is the angular velocity of joint i at time t, and $T_i(t)$ is the drive torque at each joint. However, to compare the results obtained with the simulator and with the real-robot, that has a single force torque sensor in each limbs, we approximated Eq.12 by

$$\widehat{E}(t) = \|\vec{\dot{\theta}}(t)\| \|\vec{T}(t)\|, \tag{13}$$

where $\vec{T}(t)$ is the torque data from force torque sensor available at each limb. $\vec{\dot{\theta}}(t) = \{\dot{\theta}_0(t), ..., \dot{\theta}_3(t)\}$ is the angular velocity of shoulder pitch, roll, yaw, and elbow pitch respectively. Then we sum up $\widehat{E}(t)$ after collision time t_c and get the total drive energy $\widetilde{E}$

$$\widetilde{E} = \sum_{k=t_c}^{n} \widehat{E}(t). \tag{14}$$

Table.II shows the comparison of total drive energy after collision between tonic and flexion reflex in each environments. In any case except left on flat environment, flexion reflex has better a performances to dump the impact energy than tonic reflex.

B. Real-robot Experiment

Here we describe the experiment on the generation of self-protective motions with the real robot. The RSST's parameter are set to $w = 5, n = 5$, while the sampling rate of each sensors is set to $s = 0.01\,\mathrm{sec}$. The global reaction has the chance of being elicited every $s = 0.1\,\mathrm{sec}$, the time necessary for calculating the moving average, while the local reflexes has the possibility of being elicited every $s = 0.1\,\mathrm{sec}$, the time for calculating the changing score. Because of the limitation of the hardware, we just verified that the proposed method detects the collision and elicits the local reflex. The real robot detects the contact with human and stops the limbs motion by the tonic reflex. The time sequence of force torque sensor and its change score are shown in Fig.7. The result of collision detection is shown in Fig.8.

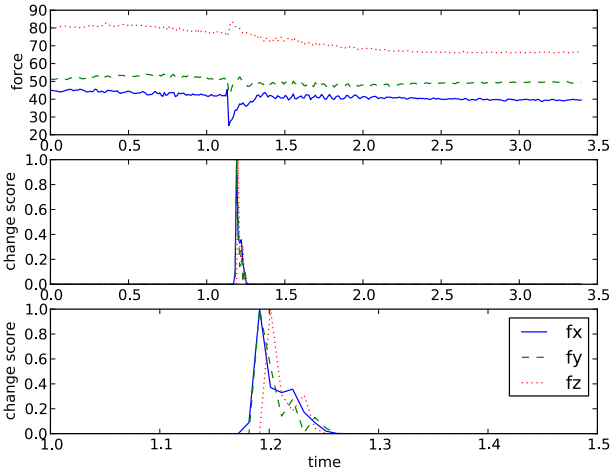

Fig. 7. The force sensor sequence of the right arm. The top is the raw sequences of each axis, the middle is the change scores and the bottom is the enlargement figure of the change score. The change scores is normalized by the local maximum.

IV. DISCUSSION

Primitive reflex[13] are known as the milestones of developmental processes of infants, thus many researchers are focused on generating the motions of robot from reflexes for achieving the human-like motion control. Nakamura et al[14] proposed the motion generation that integrates the multiple reflexes, and Yoshikai et al[15] improved the Nakamura's approach to generate the objective behaviors from multiple

TABLE II

THE COMPARISON OF THE TOTAL DRIVE ENERGY AFTER COLLISION BETWEEN TONIC AND FLEXION REFLEX IN EACH ENVIRONMENTS.

falling down direction / condition	right	half right	front	half left	left
	Flat environment				
global reaction with tonic	577.8	1821.1	574.9	2941.1	644.9
global reaction with flexion	1171.1	2164.7	2793.3	2164.1	1118.6
	Slope environment				
global reaction with tonic	498.4	918.9	408.3	2334.4	391.2
global reaction with flexion	1190.2	1806.9	2449.6	2796.6	1290.6
	Stair environment				
global reaction with tonic	713.9	526.0	757.9	1877.0	725.3
global reaction with flexion	1147.6	1738.8	2376.2	2214.8	1214.6

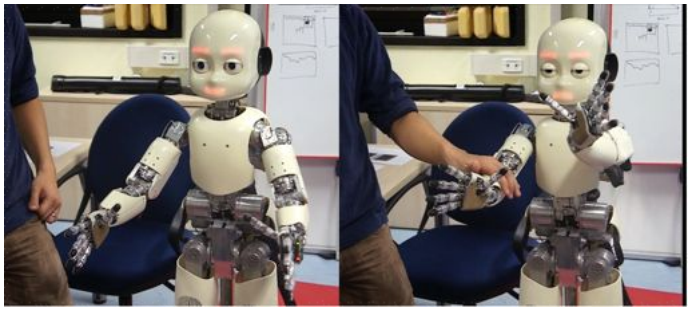

Fig. 8. Real robot experiment

reflexes. Viewed in the nervous system, these kind of motion controls is learned in the network among the cerebellum.In order to learn the effective self-protective motion, these approaches are required. Singh et al[16] proposed the novel reinforcement learning method that the instincts are motivated the learning, and this kind of system closely related to the decision making through the prefrontal cortex.Moreover, as we showed in this paper, the hierarchical structure for integrating multiple reflexes is also important for self-protective motion.As a simple comparison, the local reflex works as the spinal reflex.These hierarchical structure is required for adapting the motion to the environmental changes. Thus in order to achieve the human-like motion control, these kind of methods should be integrated for further developments of robot.

V. CONCLUSIONS

In this paper, we described the implementation for generating self-protective motion by the reflex control. We verified the effectiveness of hierarchical structure for generating self-protective motion from the global reaction and local reflexes. Our system generate the motion in real-time and dump the impact energy during falling down.

REFERENCES

[1] G. Metta, G. Sandini, D. Vernon, L. Natale, and F. Nori. The iCub humanoid robot: an open platform for research in embodied cognition. In *Proceedings of the 8th Workshop on Performance Metrics for Intelligent Systems*, pp. 50–56. ACM, 2008.

[2] R.A. Brooks. Intelligence without representation. *Artificial intelligence*, Vol. 47, No. 1-3, pp. 139–159, 1991.

[3] Q. Huang and Y. Nakamura. Sensory reflex control for humanoid walking. *Robotics, IEEE Transactions on*, Vol. 21, No. 5, pp. 977–984, 2005.

[4] G.N. Boone and J.K. Hodgins. Slipping and tripping reflexes for bipedal robots. *Autonomous robots*, Vol. 4, No. 3, pp. 259–271, 1997.

[5] K. Fujiwara, F. Kanehiro, S. Kajita, K. Kaneko, K. Yokoi, and H. Hirukawa. UKEMI: Falling motion control to minimize damage to biped humanoid robot. In *Intelligent Robots and Systems, 2002. IEEE/RSJ International Conference on*, Vol. 3, pp. 2521–2526. IEEE, 2002.

[6] Y Mohammad and T Nishida. Robust singular spectrum transform. *Next-Generation Applied Intelligence*, pp. 123–132, 2009.

[7] T. Ide and K. Inoue. Knowledge discovery from heterogeneous dynamic systems using change-point correlations. In *Proc. SIAM Intl. Conf. Data Mining*, pp. 571–575. Citeseer, 2005.

[8] N.G. Tsagarakis, G. Metta, G. Sandini, D. Vernon, R. Beira, F. Becchi, L. Righetti, J. Santos-Victor, A.J. Ijspeert, M.C. Carrozza, et al. iCub: the design and realization of an open humanoid platform for cognitive and neuroscience research. *Advanced Robotics*, Vol. 21, No. 10, pp. 1151–1175, 2007.

[9] G. Metta, P. Fitzpatrick, and L. Natale. Yarp: Yet another robot platform. *International Journal on Advanced Robotics Systems*, Vol. 3, No. 1, pp. 43–48, 2006.

[10] P. Fitzpatrick, G. Metta, and L. Natale. Towards long-lived robot genes. *Robotics and Autonomous Systems*, Vol. 56, No. 1, pp. 29–45, 2008.

[11] A. Parmiggiani, M. Randazzo, L. Natale, G. Metta, and G. Sandini. Joint torque sensing for the upperbody of the iCub humanoid robot. In *IEEE-RAS International Conference on Humanoid Robots*, 2009.

[12] V. Tikhanoff, P. Fitzpatrick, F. Nori, L. Natale, G. Metta, and A. Cangelosi. The icub humanoid robot simulator. In *IROS Workshop on Robot Simulators, September*, Vol. 22.

[13] D.I. Zafeiriou. Primitive reflexes and postural reactions in the neurodevelopmental examination. *Pediatric neurology*, Vol. 31, No. 1, pp. 1–8, 2004.

[14] Y. Nakamura, T. Yamazaki, and N. Mizushima. Motion synthesis, learning and abstraction through parameterized smooth map from sensors to behaviors. In *ROBOTICS RESEARCH-INTERNATIONAL SYMPOSIUM-*, Vol. 8, pp. 69–80. MIT PRESS, 1998.

[15] T. Yoshikai, S. Yoshida, I. Mizuuchi, D. Sato, M. Inaba, and H. Inoue. Multi-sensor guided behaviors in whole body tendon-driven humanoid Kenta. In *Multisensor Fusion and Integration for Intelligent Systems, MFI2003. Proceedings of IEEE International Conference on*, pp. 9–14. IEEE, 2003.

[16] S. Singh, A. G. Barto, and N. Chentanez. Intrinsically motivated reinforcement learning. *Advances in Neural Information Processing Systems 17*, pp. 1281 –1288, 2005.